Modified Guanines Representing O^6-Alkylation by the Cyclophosphamide Metabolites Acrolein and Chloroacetaldehyde: Synthesis, Stability, and ab Initio Studies

Narayanan Balu,[†] Michael P. Gamcsik,[†] Michael E. Colvin,[‡] O. Michael Colvin,[†] M. Eileen Dolan,[§] and Susan M. Ludeman*[,†]

Duke Comprehensive Cancer Center, Department of Medicine, Duke University Medical Center, Durham, North Carolina 27710, Biology and Biotechnology Research Program, Lawrence Livermore National Laboratory, Livermore, California 94550, and Cancer Research Center and Department of Medicine, University of Chicago, Chicago, Illinois 60637

Received September 11, 2001

Alkylation of DNA by acrolein and/or chloroacetaldehyde may result in the mutations that lead to the therapy-induced leukemia associated with cyclophosphamide (and ifosfamide) treatment. O^6-(*n*-Propanalyl)guanine (O^6-PAG) and O^6-(ethanalyl)guanine (O^6-EAG) were synthesized for use as authentic standards in investigations of DNA alkylation by acrolein and chloroacetaldehyde, respectively. Preparation of the *O*-methyl oximes of these aldehydes aided in confirming the structural assignments of O^6-PAG and O^6-EAG. HPLC was used to study the stability of O^6-PAG under a variety of conditions. The decomposition of O^6-PAG was attributed to an α,*β*-elimination reaction resulting in the formation of guanine and acrolein. In 0.1 M phosphate-DMSO (9:1), O^6-PAG (1−10 mM) had a half-life of approximately 1 h (pH 7.4, 37 °C). In 0.05 M Tris-DMSO (9:1), the apparent half-life of O^6-PAG (1−10 mM) was approximately 16 h (pH 7.4, 37 °C). The increased lifetime under the latter conditions was attributed to a reversible reaction between Tris and the aldehydic functionality of O^6-PAG to give a more stable oxazolidine. Under conditions similar to those that would be used for hydrolysis of DNA [0.1 M HCl-DMSO (98:2), pH 1.3, 70 °C, 30 min], there was an estimated 10−35% loss of O^6-PAG. Under the same conditions, O^6-EAG had apparent half-lives of 6.6 h (phosphate-DMSO) and 2.5 days (Tris-DMSO) and the estimated loss at pH 1.3 over 30 min (70 °C) was 15−20%. Ab initio quantum chemical calculations were used to understand the energy factors that underlie the occurrence of *O*- versus *N*-alkylations as well as possible, subsequent intramolecular cyclizations. Simulations of the free energies of reactions between acrolein and guanine indicated that *N*-alkylation was favored over O^6-alkylation and that cyclizations to tautomers were most favorable if they involved the N-1 or NH_2 positions.

Introduction

The anticancer agent cyclophosphamide (**1**) undergoes a sequence of metabolic transformations leading to the formation of 4-hydroxycyclophosphamide (**2**), aldophosphamide (**3**), and ultimately, phosphoramide mustard (**4**) and acrolein (**5**) (Scheme 1) (*1*). Phosphoramide mustard is responsible for cross-linking DNA (*2*) while acrolein is most commonly associated with side effects such as bladder cystitis (*3*). A competing, albeit minor (∼10%), metabolic fate of **1** results in dechloroethylation and the formation of 2-dechloroethylcyclophosphamide (**6**) and chloroacetaldehyde (**7**) (Scheme 1). The occurrence of neurotoxicity is attributed to this pathway (*4*, *5*).

Recently, we provided the first evidence that O^6-alkylguanine-DNA alkyltransferase (AGT) plays an important role in protecting against the toxicity and mutagenicity of **1** (*6*, *7*). We also demonstrated that this relationship between AGT and **1** is specifically correlated with acrolein and not phosphoramide mustard (*7*). Considering that AGT repair of DNA involves removal of an alkyl group from the O^6 position in a guanine residue, two pathways were presented by which acrolein might generate such a repairable adduct. Acting as a nucleophile, the guanylic oxygen could initiate a conjugate

Scheme 1

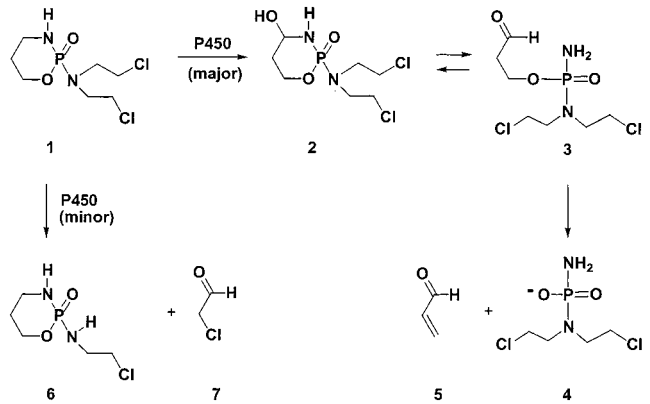

* To whom correspondence should be addressed. Phone: (919) 681-2808. Fax: (919) 684-5653. Email: s.ludeman@duke.edu.
[†] Duke Comprehensive Cancer Center and Department of Medicine, Duke University Medical Center.
[‡] Lawrence Livermore National Laboratory.
[§] University of Chicago.

10.1021/tx0101503 CCC: $22.00
Published on Web 02/08/2002

Scheme 2[a]

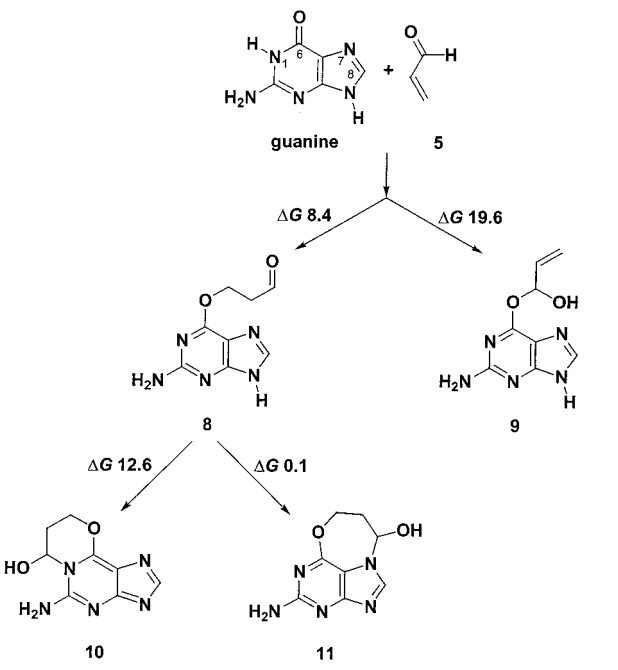

[a] ΔG in kcal/mol, COSMO method.

Scheme 3[a]

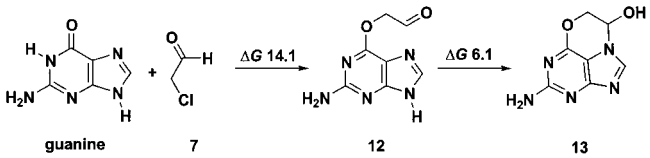

[a] ΔG in kcal/mol, COSMO method.

addition across the α,β-unsaturated system of acrolein and/or it could directly add across the aldehydic moiety of acrolein (*6*). The products given by these two mechanisms are depicted as O^6-alkylated guanines **8** and **9**, respectively, in Scheme 2. Considering the general reactivity of α,β-unsaturated aldehydes, **8** is expected to be the thermodynamic product and **9** the kinetic product (*8*). Thus, even though an adduct such as **9** might form faster than **8**, it is anticipated that **9** would be unstable due to the predicted lability of the hemiacetal moiety. In fact, reactions between acrolein and different nitrogens in guanine, guanosines, and guanyl residues in DNA have led almost exclusively to the isolation of the thermodynamic products derived from conjugate addition (*9*-*17*). On the other hand, a Schiff base adduct between crotonaldehyde ($CH_3CH{=}CHCHO$) and the exocyclic NH_2 of a guanyl residue in DNA has recently been reported, and this would be the result of an initial, direct addition of the amine across the aldehydic carbonyl (*18*).

The reactivity of chloroacetaldehyde (**7**) toward substitution reactions (with loss of chloride) suggests that this is another cyclophosphamide metabolite capable of alkylating nucleophilic sites in DNA, including the O^6 position of a guanine residue. By way of comparison, O^6-allylguanine has been reported as a product derived from the alkylation of DNA by allyl chloride ($ClCH_2CH{=}CH_2$), a compound with chemical properties somewhat similar to those of **7** (*19*).

Alkylation of DNA by acrolein and/or chloroacetaldehyde may result in the mutations that lead to the therapy-induced leukemia associated with cyclophosphamide treatment. Recent mutagenicity studies of oligonucleotides containing the major adduct formed from *N*-alkylation of guanine by acrolein suggest that this lesion is not likely to be responsible for the mutagenic effects associated with acrolein (*17*). While the formation of chloroacetaldehyde derives from a minor metabolic pathway for cyclophosphamide, it accounts for approximately half of the metabolic fate of the related anticancer agent ifosfamide (*4*, *5*). Thus, a determination of the total contributions of these metabolites to the toxicity and mutagenicity of the oxazaphosphorines remains an area of active research.

For the purpose of identifying mutagenic lesions in DNA caused by acrolein and chloroacetaldehyde, authentic adducts are needed as standards. Herein, we report the synthesis of the thermodynamic product resulting from O^6-alkylation of guanine by acrolein, O^6-(*n*-propanalyl)guanine (**8**; "O^6-PAG", Scheme 2). Also included are studies of the chemical stability of **8** under conditions used for DNA incubation and digestion. Quantum chemical calculations are presented that compare the relative favorabilities of O^6-alkylated adducts such as **8** and **9** with *N*-alkylated guanines. We also report the synthesis and study of O^6-(ethanalyl)guanine (**12**; "O^6-EAG", Scheme 3) as representative of the adduct formed from O^6-alkylation of a guanine moiety in DNA by chloroacetaldehyde.

Experimental Procedures

In general, reagents were purchased from Aldrich Chemical Co., Milwaukee, WI, and were used without further purification. Reactions that did not include water were carried out under a slight positive pressure of nitrogen. Melting points were determined with a Fisher-Johns melting point apparatus and are uncorrected. A Labconco Freeze-Dry System/Freezone 4.5 was used for lyophilizing samples. ^{1}H (300 MHz) and ^{13}C NMR (75 MHz) were recorded on a Varian Mercury-300 spectrometer. Samples were dissolved in DMSO-d_6 containing 0.1% TMS as an internal standard. Flash chromatography used 230−400 mesh silica gel (Merck). Preparative TLC used silica gel 60 F_{254} (Merck), 0.25, 0.5, and 1 mm plates (20 × 20 cm). The maximum amount of crude product applied to each plate was approximately 25, 50, and 100 mg, respectively. Component visualization was made using a UV lamp.

High-resolution fast atom bombardment (FAB) mass spectra were obtained using a JEOL JMS SX-102 mass spectrometer. Data were acquired in the scanning mode using a matrix mixture of *m*-nitrobenzyl alcohol and PEG-600. Masses were acquired 200 amu above and below the predicted mass of the analyte.

HPLC analyses were conducted on a Waters (Milford, MA) system equipped with a 996-Photodiode Array Detector, 474-Scanning Fluorescence Detector, 515-HPLC Pumps and 717-plus Autosampler interfaced with Waters Millennium^{32} Chromatography Manager Software. Some fluorescence spectra were also recorded on a Shimadzu RF 1501 spectrometer. Some UV spectra were also recorded on a Beckman DU-600 spectrophotometer.

***O*^{6}-(3-Butenyl)guanine (14).** With modifications to published syntheses of analogous compounds (*20*−*22*), freshly cut metallic sodium (5.9 mmol, 0.14 g) was added slowly to neat 3-buten-1-ol (35 mmol, 3.0 mL) at 50 °C. When the sodium was no longer visible (∼10 min), 2-amino-6-chloropurine (3.0 mmol, 0.50 g) was added and the mixture was heated at 110 °C for 10 h. The excess 3-buten-1-ol was removed by distillation and the residue was flash chromatographed on silica gel (3 cm × 47 cm column) using $CHCl_3$−CH_3OH (3:1) to obtain the product as a white, crystalline solid [2.7 mmol, 0.56 g, 90% yield, mp 195−198 °C, R_f 0.68 in $CHCl_3$-CH_3OH (3:1)]. ^{1}H NMR (DMSO-d_6) δ

12.42 (br s, 1H, exchangeable with D_2O, NH), 7.82 (s, 1H, C-8 proton), 6.23 (s, 2H, exchangeable with D_2O, NH_2), 5.86 (ddt, J = 7, 10 and 17 Hz, 1H, C***H***=CH_2), 5.22−5.07 (m, 2H, CH=C***H***$_2$), 4.43 (t, 2H, J = 7 Hz, OCH_2), and 2.54 [apparent dt, J = 7 and 7 Hz (plus 1 Hz fine splitting), 2H, OCH_2C***H***$_2$]. ^{13}C NMR (DMSO-d_6) δ 159.5 (C-2 and C-6), 154.8 (C-4), 137.44 (C-8), 134.5 (***C***H=CH_2), 117.0 (CH=***C***H_2), 113.4 (C-5), 64.50 (OCH_2), and 32.87 (OCH_2***C***H_2). MS (FAB$^+$) m/z calcd for $C_5H_{12}N_5O$ $[M + H]^+$ 206.1043, found 206.1042.

O*^{6}-(*n*-Propanalyl)guanine (8; *O*^{6}-PAG).** Solid OsO_4 (1.0 mmol, 0.25 g) was added to a solution of butenyl guanine adduct **14** (0.20 g, 1.0 mmol) in CH_3OH-H_2O (3:1, 5 mL). The mixture was stirred for 10−15 min and then solid $NaIO_4$ (1.5 mmol, 0.31 g) was added (*23*). After 1 h, the reaction mixture was vacuum filtered through a fritted glass funnel, and the solids were washed (CH_3OH). The filtrate was concentrated on a rotary evaporator, and the residue was placed under high vacuum. Residual water was removed on a freeze-dryer and the crude product was obtained as a solid (94 mg, ∼0.45 mmol, yield ∼45%). MS (FAB$^+$) m/z calcd for $C_8H_{10}N_5O_2$ $[M + H]^+$ 208.0835, found 208.0835. ^{1}H NMR (DMSO-d_6/D_2O, ca. 2:1) δ 9.8 (CHO), 8.1−7.8 (C-8 proton), 4.7−4.1 (m, OCH_2), and CH***$_2$CHO obscured by DMSO-d_5 or HOD. Possible proton signals due to contributions from an aldehyde hydrate were obscured by the HOD resonance.

Crude product was dissolved in CH_3OH-$CHCl_3$ (1:1) and filtered. HPLC analysis of this solution showed one major peak with diode array UV spectra indicating λ_{max} = 293 nm with a shoulder at 235 nm. The major peak was the only one that was visible by fluorescence detection [in CH_3CN (ca. 1 mg in 10 mL), 294 (excitation) and 353 (emission) nm].

E/Z*−*O*^{6}-(*n*-Propanalyl)guanine *O*-Methyloxime (*E/Z*-15; *E/Z*-*O*^{6}-PAG-oxime).** *O*-Methylhydroxylamine hydrochloride (0.45 mmol, 38 mg) was dissolved in 0.2 M NaOH (1 mL), and the pH of the solution was then adjusted to 7.4. This was added to a solution of *O*^{6}-PAG (**8**; ∼0.45 mmol, 94 mg) in DMSO (0.5 mL), and the mixture was stirred for 3 h. The reaction mixture was concentrated on a freeze-dryer, and the residue was purified by preparative TLC on silica gel using $CHCl_3$-CH_3OH (7:3). While the *E*- and *Z*-stereoisomers were observed at different R_f values (0.7 and 0.6), the two bands on the preparative plates were collected together. Product was desorbed from silica gel using $CHCl_3$-CH_3OH (1:1), and **15** was obtained as a white solid in 56% yield (0.25 mmol, 59 mg, 56% *E* and 44% *Z*-isomers, mp range 165−195 °C with decomposition over 200 °C). Signal assignments and isomer composition by ^{1}H NMR were based on literature reports of spectral data for similar oximes (*24*). ^{1}H NMR (DMSO-d_6) δ 12.40 (br s, 1H, exchanges with D_2O, NH), 7.78 (s, 1H, C-8 proton), 7.45 (t, J = 6 Hz, 0.56 H, ON=CH of *E*-isomer), 6.85 (t, J = 5 Hz, 0.44 H, ON=CH of *Z*-isomer), 6.20 (s, 2H, exchangeable with D_2O, NH_2), 4.50 (*E*) and 4.48 (*Z*) [two t, J = 7 (*E*) and 6 (*Z*) Hz, 2H total, OCH_2], 3.75 (*Z*) and 3.69 (*E*) [two s, 3H total, OCH_3] and 2.69 (*Z*) and 2.59 (*E*) [two apparent q, J = 6 (*Z*) and 6 (*E*) Hz, 2H total, OCH_2CH***$_2$]. ^{13}C NMR (DMSO-d_6) δ 159.5 (C-2 and C-6), 156.31 (C-4), 148.4 and 148.1 (*E*/*Z* C=NO), 138.0 (C-8), 112.4 (C-5), 62.43, 62.29, 61.18, and 60.78 (*E*/*Z* OCH_2 and OCH_3), and 29.07 and 25.80 (*E*/*Z* ***C***H_2C=N). MS (FAB$^+$) m/z calcd for $C_9H_{13}N_6O_2$ $[M + H]^+$ 237.1101, found 237.1107. UV (0.5 mg of product in 7.5 mL of CH_3CN and diluted with 7.5 mL of H_2O): 282 and 240 nm; the extinction coefficient at 282 nm was 7667 $M^{-1}cm^{-1}$ (mixture of isomers). Fluorescence in CH_3CN (ca. 1 mg in 10 mL): 286 (excitation) and 348 (emission) nm.

O*^{6}-(Allyl)guanine (16).** With minor modifications to published procedures (*19*, *20*, *25*), freshly cut metallic sodium (11.8 mmol, 0.14 g) was added slowly to neat allyl alcohol (118 mmol, 8.0 mL) at room temperature. When the sodium was no longer visible (∼10 min), 2-amino-6-chloropurine (5.9 mmol, 1.0 g) was added, and the mixture was heated at 100 °C for 10 h. The excess allyl alcohol was removed by distillation, and the residue was flash chromatographed on silica gel (3.5 cm × 37 cm) using $CHCl_3$−CH_3OH (3:1) to obtain the product as a white, crystalline solid [5.2 mmol, 1.0 g, 88% yield, mp 205−207 °C, R_f 0.63 in $CHCl_3$-CH_3OH (7:1)]. ^{1}H NMR (DMSO-d_6) δ 12.44 (br s, 1H, exchangeable with D_2O, NH), 7.84 (s, 1H, C-8 proton), 6.24 (s, 2H, exchangeable with D_2O, NH_2), 6.23−6.03 (m, 1H, CH***=CH_2), 5.49−5.23 (m, 2H, CH=C***H***$_2$), and 5.00 (d, 2H, J = 1.4 Hz, OCH_2). ^{13}C NMR (DMSO-d_6) δ 160.2 (C-2 and C-6), 155.7 (C-4), 138.4 (C-8), 134.1 (***C***H=CH_2), 118.6 (CH=***C***H_2), 114.1 (C-5), and 66.57 (OCH_2). MS (FAB$^+$) m/z calcd for $C_8H_{10}N_5O$ $[M + H]^+$ 192.0886, found 192.0886. Diode array UV spectra indicated λ_{max} = 281 nm with another peak at 240 nm.

***O*^{6}-(Ethanalyl)guanine (12, *O*^{6}-EAG).** The title compound was synthesized exactly as described for **8** using solid OsO_4 (1.57 mmol, 0.40 g) and propenyl guanine adduct **16** (1.57 mmol, 0.30 g) in CH_3OH-H_2O (3:1, 10 mL). The mixture was stirred for 15 min, solid $NaIO_4$ (2.36 mmol, 0.50 g), was added and stirring was continued for 1 h (*23*). Following a workup as described for **8**, the lyophilized material was taken up in CH_3OH-$CHCl_3$ (1:1) and filtered; the clear filtrate was concentrated on a rotary and then under high vacuum. The crude product was obtained as an off-white solid (80 mg, ∼0.42 mmol, ∼26% yield, mp >250 °C). MS (FAB$^+$) m/z calcd for $C_7H_8N_5O_2$ $[M + H]^+$ 194.0679, found 194.0674. ^{1}H NMR (DMSO-d_6/D_2O, ca. 2:1) δ 9.7 (CHO), 7.8 (C-8 proton), and 4.8 (OCH_2). Possible proton signals due to contributions from an aldehyde hydrate were obscured by the HOD resonance. Diode array UV spectra indicated λ_{max} = 280 nm with another peak at 239 nm.

***E/Z*−*O*^{6}-(*n*-Ethanalyl)guanine *O*-Methyloxime (*E/Z*-17; *E/Z*-*O*^{6}-EAG-oxime).** The title compound was made and purified as described for *E*/*Z*-**15** using *O*-methylhydroxylamine hydrochloride (0.21 mmol, 17 mg) in 0.2 M NaOH (1.5 mL) and *O*^{6}-EAG (**12**; ∼0.21 mmol, 40 mg) in DMSO (0.5 mL). Product **17** was obtained as a white solid in 19% yield [0.04 mmol, 10 mg, 35% *E*- and 65% *Z*-isomers, R_f 0.65 in $CHCl_3$-CH_3OH (7:3), mp 200−206 °C]. Signal assignments and isomer composition by ^{1}H NMR were based on literature reports of spectral data for similar oximes (*24*). ^{1}H NMR (DMSO-d_6) δ 12.47 (br s, 1H, exchangeable with D_2O, NH), 7.86 (s, 1H, C-8 proton), 7.72 (apparent t, J = 6 Hz, 0.35 H, ON=CH of *E*-isomer), 7.11 (apparent t, J = 4 Hz, 0.65 H, ON=CH of *Z*-isomer), 6.31 (br s, 2H, exchangeable with D_2O, NH_2), 5.16 (*Z*) and 4.98 (*E*) [two d, J = 4 (*Z*) and 6 (*E*) Hz, 2H total, OCH_2], and 3.86 (*Z*) and 3.80 (*E*) (two s, 3H total, OCH_3). ^{13}C NMR (DMSO-d_6) δ 159.4 (C-2 and C-6), 155.4 (C-4), 148.5 and 146.2 (*E*/*Z* C=NO), 138.3 (C-8), 113.2 (C-5), and 61.96, 61.55 and 60.01 (*E*/*Z* OCH_2 and OCH_3). MS (FAB$^+$) m/z calcd for $C_8H_{11}N_6O_2$ $[M + H]^+$ 223.0944, found 223.0944. Diode array UV spectra indicated λ_{max} = 281 nm with another peak at 239 nm.

Kinetics. In general, samples were analyzed at 1-h intervals using an HPLC unit with an auto-injector and temperature control. At each time point, chromatograms were generated using UV and fluorescence detectors. Peak areas (using, in general, fluorescence detection) were used to measure relative concentrations of components as a function of time. Linear least-squares fits of pseudo-first-order plots of the disappearance of individual HPLC peaks provided the half-lives given in Table 1.

Phosphate-DMSO. An appropriate weight of the compound of interest was dissolved in DMSO (0.1 mL) and this was then diluted with 0.9 mL of 0.1 M phosphate buffer (potassium phosphate monobasic) at pH 7.4. After mixing, the pH was readjusted to 7.4.

Tris-DMSO. A buffer was prepared which was 50 mM in Tris, 0.1 mM in EDTA and 5 mM in dithiothreitol and the pH was adjusted to 7.4. An appropriate weight of the compound of interest was dissolved in DMSO (0.1 mL) and this was then diluted with 0.9 mL of the Tris buffer. The pH was readjusted to 7.4.

0.1 M HCl-DMSO. An appropriate amount of *O*^{6}-PAG (**8**) or *O*^{6}-EAG (**12**) was dissolved in DMSO (0.05 mL) and this was diluted with 0.1 M HCl (2.95 mL). The solution was mixed, and an aliquot (0.5 mL) was analyzed immediately by HPLC. The remaining solution was heated to 70 °C, and aliquots were taken

Table 1. Solution Stability of O^6-PAG (8), O^6-EAG (12) and O^6-PAG-Oxime (15)

compd	concentration (mM)	solution	pH; temp	stability[a]
8	1	0.1 M phosphate-DMSO (9:1)	7.4; 37 °C	$\tau_{1/2} = 57$ min (0.998)[b]
8	5	0.1 M phosphate-DMSO (9:1)	7.4; 37 °C	$\tau_{1/2} = 53$ min (0.999)[b]
8	10	0.1 M phosphate-DMSO (9:1)	7.4; 37 °C	$\tau_{1/2} = 57 \pm 9$ min (0.994 ± 0.003)[b,c]
15	5	0.1 M phosphate-DMSO (9:1)	7.4; 37 °C	no loss over 18 h[d]
8	1	50 mM Tris[e] - DMSO (9:1)	7.4; 37 °C	$\tau_{1/2} = 15 \pm 2$ h (0.993 ± 0.001)[c,d,f]
8	8	50 mM Tris[e]-DMSO (92:8)	7.4; 37 °C	$\tau_{1/2} = 16$ h (0.995)[d,f,g]
8	10	50 mM Tris[e]-DMSO (9:1)	7.4; 37 °C	$\tau_{1/2} = 17$ h (0.993)[d,f]
8	5	DMSO	[h]; RT	$\tau_{1/2} = 46$ h (0.960)[d]
8	0.8	0.1 M HCl-DMSO (98:2)	1.3; 70 °C	10−15% loss/30 min[i]
8	1.6	0.1 M HCl-DMSO (98:2)	1.3; 70 °C	35% loss/30 min[i]
12	5	0.1 M phosphate-DMSO (9:1)	7.4; 37 °C	$\tau_{1/2} = 6.6$ h (0.999)[d]
12	5	50 mM Tris[e]-DMSO (9:1)	7.4; 37 °C	$\tau_{1/2} = 2.5$ days (0.732)[d,f]
12	0.8	0.1 M HCl-DMSO (98:2)	1.3; 70 °C	15−20% loss/30 min[g,i]
12	1.6	0.1 M HCl-DMSO (98:2)	1.3; 70 °C	15% loss/30 min[g,i]

[a] Half-lives were determined using HPLC and fluorescence detection to measure changes in peak area with time. Numbers in parentheses are correlation coefficients. In general, experimental error limits are estimated at ±15%. [b] Kinetic data derived from time points taken hourly over 4−5 h. [c] Average of two runs. [d] Kinetic data derived from time points taken hourly over 14−24 h. [e] Buffer also contained EDTA and dithiothreitol (see Kinetics section in the Experimental Procedures for details). [f] In Tris, aldehydes **8** and **12** likely participate in a pseudo-equilibrium with a more stable oxazolidine. Thus, the given values are 'apparent half-lives' (see Adduct Stabilities in text for details). [g] UV detection was used to measure peak areas. [h] Ambient pH. [i] Stability determined through '2 point' kinetic plots (change in concentration between 30 and 60 min of reaction time). A high degree of uncertainty is associated with these determinations.

Scheme 4

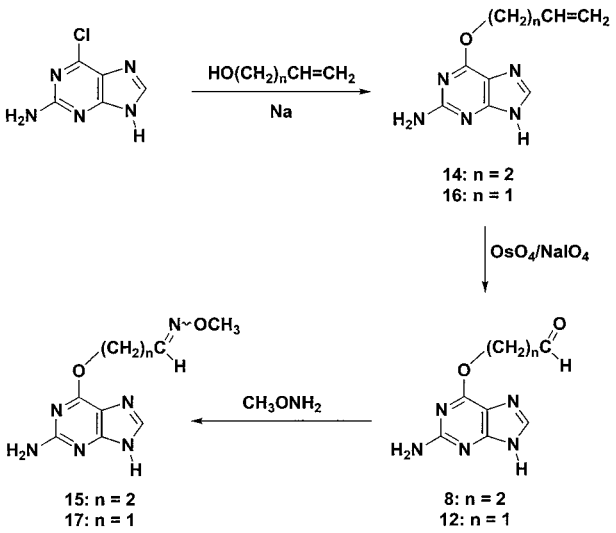

at 0.5 and 1 h intervals and kept frozen (−20 °C) until HPLC analysis.

HPLC Method and Data. Compounds were separated on a Waters Spherisorb S5 ODS2 reverse phase column (4.6 mm × 250 mm) using a gradient mobile phase of deionized water and acetonitrile, starting with 100% deionized water and increasing linearly to 30% acetonitrile over 30 or 40 min, then increasing linearly to 80% acetonitrile over 10 min and equilibrating back to 100% water over 10 min. The flow rate was 1 mL/min and the column was at room temperature. Compounds were monitored by (1) fluorescence detection at $\lambda_{excitation} = 295$ nm and $\lambda_{emission} = 375$ nm using a Waters 474-Scanning Fluorescence Detector and (2) UV detection at 290 nm using a Waters 996-Photodiode Array Detector. Using the gradient where acetonitrile was increased from 0 to 30% over 30 min, the following retention times (±1 min) were obtained: **8** (O^6-PAG), 19 min; **14**, 39 min; **15** (O^6-PAG-oxime), 27 min; and **16**, 27 min. Using the gradient where acetonitrile was increased from 0 to 30% over 40 min, the following retention times were obtained: **8** (O^6-PAG), 20 ± 2 min; **15** (O^6-PAG-oxime), 35 ± 3 min; **12** (O^6-EAG), 17 ± 1 min; and **17** (O^6-EAG-oxime), 28 ± 1 min.

Quantum Chemical Calculations. The structures of all compounds were optimized in the gas-phase using density functional theory DFT with the Becke three parameter exchange (*26*) and Lee−Yang−Parr correlation functional (B3LYP) (*27*) with a 6-31+G(d,p) basis set (*28*), an approach that has been widely demonstrated to yield accurate chemical structures and reaction energies for most molecules (*29*). The molecular entropies and thermal corrections to the free energies were calculated from the harmonic vibrational constants determined by analytic energy second derivatives calculated at the gas-phase optimized structures.

To estimate the effect of aqueous solvation on the relative energies, single point energies were calculated at the B3LYP optimized geometries using a dielectric continuum solvation model [COSMO (*30*)] coupled to the DFT B3LYP wave function. This method has been shown to yield accurate solvation energies for a wide range of compounds. In general, the use of gas-phase optimized molecular structures in the calculation of solution-phase energies has been found to yield relative energies in very good agreement with those calculated from solution-phase optimized structures (*30*−*33*). Additionally, the solvation energies were calculated using an independent model, the Langevin Dipole method (*34*), which approximates the surrounding aqueous medium as a series of point dipoles fixed to a grid. The Langevin Dipole solvation energies were calculated using ChemSol 2.1 (*34*), using Merz−Kollman (*28*) atomic charges derived from the B3LYP/6-31G (34) wave function using the polarizable continuum model (*35*). Overall, there was good agreement between the solvation energies calculated by the COSMO and ChemSol methods. All other calculations were performed using Gaussian 98 (*36*).

Results and Discussion

Synthesis and Identification of Adducts O^6-PAG (8) and O^6-EAG (12). Acrolein adduct O^6-PAG (**8**) was synthesized using variations on literature procedures for other O^6-derivitized guanines (*19-22*, *25*). As shown in Scheme 4, reaction of the sodium salt of 3-buten-1-ol with 2-amino-6-chloropurine gave intermediate **14**. Oxidative cleavage (*23*) of the alkene functionality in **14** provided the desired aldehyde, O^6-PAG (**8**). ^{1}H NMR spectra of the crude product showed a signal indicative of an aldehydic proton; resonances for an alkene moiety were absent. HPLC analysis using UV detection gave one major and several small peaks, suggesting the presence of minor impurities and/or equilibrium structures (e.g., **10** and/or **11**, Scheme 2), which will be discussed in a later section. The major product visible by UV was the only component to give an intense signal upon detection with fluorescence [a characteristic of O^6- but not N-alkylated derivatives of guanines (*37*)].

Due to the fact that chromatographic (silica gel and reverse phase) purifications of O^6-PAG were unsatisfactory, the structural integrity of this compound was established by generating a derivative of **8** with *O*-methylhydroxylamine. The resultant oxime was much more stable than its aldehydic precursor and, therefore, was readily chromatographed and characterized (NMR, MS) as compound **15**, the *E*- and *Z*-isomers of the *O*-methyl oxime of O^6-PAG (Scheme 4). When the oxime reaction was followed by HPLC, the peak assigned to O^6-PAG rapidly disappeared upon addition of *O*-methylhydroxylamine. This was accompanied by the appearance of a peak attributable to oxime **15** (as identified with authentic material).

As shown in Scheme 4, O^6-EAG (**12**) was made by a pathway parallel to that for O^6-PAG with the previously reported O^6-allyl **16** as the intermediate (*20*, *25*). In the ^{1}H spectrum of **16**, the presence of a singlet at δ 7.84 for the C-8 proton was particularly useful in determining the isomeric integrity of this compound. It has been shown that **16** and related O^6-allylguanines are subject to a rearrangement wherein the allylic group shifts from the O^6 to the C-8 position; however, this rearrangement can be suppressed with appropriate control of temperature and reaction times (*37*).

Oxidation (*23*) of **16** provided O^6-EAG (**12**) and, as with O^6-PAG, this compound was difficult to isolate in pure form. Crude O^6-EAG showed an aldehyde resonance by proton NMR and a major component by HPLC that displayed strong fluorescence. As with O^6-PAG, the possibility of O^6-EAG interconverting with one or more tautomers was considered (e.g., **13**, Scheme 3), as discussed in a later section. Conversion of **12** to an oxime with *O*-methylhydroxylamine provided the more stable and readily characterized *E*/*Z*-**17**, the diastereomeric *O*-methyl oximes of O^6-EAG (Scheme 4). As with O^6-PAG, the oxime reaction was followed by HPLC. Addition of *O*-methylhydroxylamine resulted in the disappearance of the peak assigned to O^6-EAG concomitant with the appearance of a signal for oxime **17**.

Adduct Stabilities. The stability of O^6-PAG (**8**) was studied under a variety of conditions using HPLC to monitor changes in component concentration (Table 1). The loss of O^6-PAG was accompanied by the appearance of guanine as identified through the use of authentic material. The formation of guanine (and acrolein) could be accounted for by an α,β-elimination reaction initiated by base-catalyzed removal of a proton α to the carbonyl in **8**. On the basis of this likely mechanism, it could be predicted that the decomposition of O^6-PAG would be dependent on a variety of conditions including buffer-type and pH. Such condition-dependent rates are known for aldophosphamide (**3**) which undergoes an analogous α,β-elimination to give acrolein and phosphoramide mustard (**4**, Scheme 1) (*1*, *38*-*42*).

If the fragmentation of O^6-PAG to guanine and acrolein were reversible, the rate of reaction would also be dependent on the concentrations of the reactants. Within experimental error limits ($\pm$15%), no such dependency was observed in these kinetic studies; however, no precautions were taken to prevent or minimize the loss of the volatile acrolein from the reaction mixture. Thus, the half-lives given in Table 1 reflect irreversible fragmentation rates but that may be a function of experimental design.

As shown in Table 1, the apparent lifetime of O^6-PAG in Tris is much longer than that in phosphate. This is not surprising in view of the fact that Tris is known to effectively enhance the stability of aldophosphamide (**3**) (*38*, *39*). In a reversible reaction, Tris adds across the aldehydic functionality in **3** and, presumably, in O^6-PAG to give an oxazolidine product (*38*, *39*). The loss of the carbonyl moiety decreases the acidity of the hydrogens on the adjacent methylene group and this disfavors any α,β-elimination reaction of the oxazolidine. In the interconversion of the aldehydic species and the oxazolidine, higher concentrations of Tris favor the oxazolidine and, conversely, lower concentrations favor the aldehyde. Thus, injection of the O^6-PAG/Tris reaction mixture onto an HPLC column (using Tris-free eluent) results in a significant dilution of Tris, and the pseudo-equilibrium between oxazolidine and aldehyde shifts to greatly favor O^6-PAG. The free aldehyde (or its hydrate) is the species that is then detected. While Tris is likely the major contributor to the rate retardation seen in these experiments, the presence of dithiothreitol in this buffer may also play some role. Again, with aldophosphamide, thiols are known to add in a reversible manner across the aldehydic moiety producing more stable hemithioacetals (*1*, *38*, *43*). The apparent stability of O^6-PAG in this particular Tris buffer system (containing EDTA and dithiothreitol) was of particular interest because we have used it for past studies of DNA alkylation (*7*, *44*) and we expect to use it for future investigations of O^6-guanyl alkylation by acrolein. The good stability of O^6-PAG (via its oxazolidine) under these conditions suggests that if such an adduct is formed in DNA, it should convert to the oxazolidine and, therefore, survive long enough to be detected.

Under conditions similar to those used in DNA digestion (0.1 M HCl, 70 °C, 30 min), O^6-PAG was reasonably stable with an estimated decomposition rate of 10−35%/30 min (Table 1). A high degree of uncertainty was associated with these determinations as each kinetic plot employed just two time points. Nevertheless, it was clear from the chromatograms that a substantial portion of the starting material survived the hydrolysis conditions. Assuming that the major loss of O^6-PAG was a result of base-catalyzed elimination, it was consistent that acidic conditions would favor stability, even at the temperature extreme of 70 °C.

Aldophosphamide (**3**) is readily converted to stable oximes through reactions with hydroxylamines (*24*, *45*). In anticipation that this chemistry might have some applications to the ultimate goal of detecting O^6-alkylated residues in DNA, the stability of the *O*-methylhydroxyloxime of O^6-PAG (**15**) was studied in a limited manner. HPLC analyses of solutions of **15** at pH 7.4 in phosphate/DMSO showed no signs of decomposition over 18 h at 37 °C (Table 1).

Under similar conditions, O^6-EAG (**12**) was more stable than O^6-PAG (Table 1) but, as with O^6-PAG, the loss of O^6-EAG was accompanied by the appearance of guanine. The likely mechanism of decomposition for O^6-EAG is an irreversible substitution reaction whereby a nucleophile attacks the carbon adjacent to the carbonyl resulting in the formation of an α-substituted acetic acid and the liberation of guanine. The rate of displacement can be modulated by various factors including nucleophile strength (e.g., water versus phosphate versus Tris) and changes in the electrophilicity and accessibility of the

Scheme 5[a]

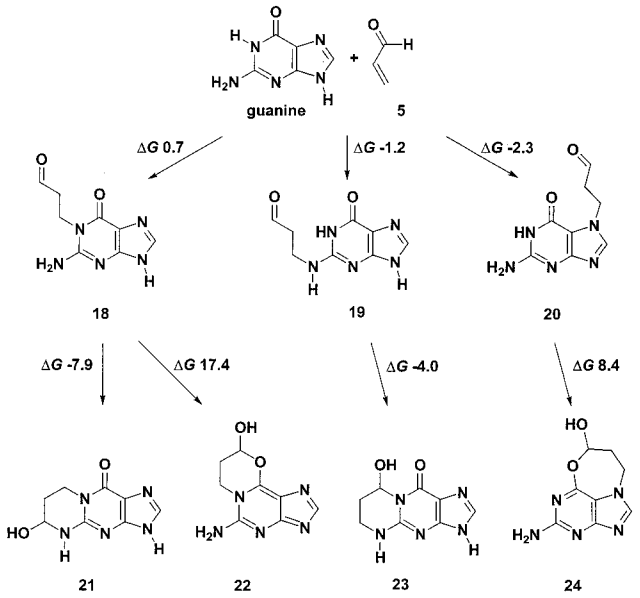

[a] ΔG in kcal/mol, COSMO method.

alpha carbon (as in conversion of the carbonyl to an oxazolidine with Tris).

Ab Initio Studies of *O*- versus *N*-Alkylations and Tautomer Formation. To date, the major products isolated from reactions between acrolein and guanine (or deoxyguanosine) arise from conjugate addition at the N-1 (**18**) and, especially, the exocyclic NH_2 (**19**) positions on the guanyl ring (Scheme 5). Each of these adducts is isolated as its more stable tautomer derived from intramolecular cyclization: **18** → **21** and **19** → **23** (Scheme 5) (*9*, *10*, *15*). The formation of similar tautomeric structures was considered for O^6-PAG (**8**) and O^6-EAG (**12**), but no experimental evidence was obtained to support the occurrence of any such reactions (Scheme 2, **8** → **10** and/or **11**; Scheme 3, **12** → **13**).

To enhance our experimental studies of alkylated guanines, ab initio quantum chemical calculations were used to understand the energy factors that underlie the occurrence of *O*- versus *N*-alkylations as well as possible, subsequent intramolecular cyclizations (Tables 2 and 3; Schemes 2, 3, and 5). For each reaction of interest, the reaction free energy was calculated using quantum chemical density functional methods and including aqueous solvation effects using implicit solvent models (COSMO and ChemSol, see Experimental Procedures for details).

For guanine-acrolein and guanine-chloroacetaldehyde adducts, relative enthalpies and free energies in the gas phase as well as relative free energies in the aqueous phase (COSMO and ChemSol methods) are given in Table 2. Reaction free energies for each alkylation and subsequent cyclization reaction are given in Table 3 (both gas and aqueous phase, Cosmo and ChemSol methods). Because the COSMO method is currently believed to give the most accurate solvation energies, these are the numbers reported in Schemes 2, 3, and 5. In all cases, a lower (or more negative) energy indicates a more favored structure (Table 2) or reaction (Table 3 and the schemes). The reaction free energies indicate which reactions are thermodynamically favored, and therefore, they predict the equilibrium distribution of products. If, however, there are significant energy barriers to these reactions, a different product distribution may be kinetically favored.

Table 2. Relative Energies of the Guanine-Acrolein and Guanine-Chloroacetaldehyde Adducts[a]

	gas phase[b]		aqueous phase	
			COSMO	ChemSol
	ΔH	ΔG^c	ΔG^d	ΔG^e
compd	(kcal/mol)	(kcal/mol)	(kcal/mol)	(kcal/mol)
8	8.91	7.20	10.71	11.35
9	18.25	17.89	21.85	24.04
18	0.00	0.00	2.95	2.65
19	4.04	3.36	1.07	−3.38
20	0.91	−0.45	0.00	0.00
10	34.57	34.45	28.21	23.43
11	16.82	16.57	15.74	14.66
21	2.58	1.72	0.00	0.00
22	31.02	30.66	25.32	20.24
23	0.00	0.00	2.03	1.28
24	12.79	12.65	13.34	11.24
12	0.00	0.00	0.00	0.00
13	9.21	11.27	6.14	9.07

[a] Energies are computed relative to the most stable isomer among the monofunctional and cyclic subsets of adducts. [b] Gas-phase energies calculated at the B3LYP/6-31+G (*28*) level of theory. [c] All energies were calculated at the gas-phase B3LYP/6-31+G (*28*) optimized geometries. Thermal enthalpy corrections and entropy terms were calculated from the B3LYP/6-31+G (*28*) harmonic vibrational frequencies. [d] Calculated using the conductor-like screening solvation model (COSMO) using the B3LYP/6-31+G (*28*) wave function. [e] Calculated using the Langevin Dipole solvent model (*34*) (ChemSol) using Merz−Kollman (*28*) atomic charges derived from the B3LYP/6-31G (*34*) wave function using the polarizable continuum model (*35*).

Table 3. Energies of the Reactions Involving the Formation of Guanine-Acrolein(5) and Guanine-Chloroacetaldehyde(7) Adducts

	gas phase[a]		aqueous phase	
			COSMO	ChemSol
	ΔH	ΔG^b	ΔG^c	ΔG^d
reaction	(kcal/mol)	(kcal/mol)	(kcal/mol)	(kcal/mol)
guanine + **5** → **8**	−11.07	0.91	8.42	11.81
guanine + **5** → **9**	−1.73	11.60	19.56	24.50
guanine + **5** → **18**	−19.98	−6.29	0.66	3.11
guanine + **5** → **19**	−15.93	−2.92	−1.23	−2.92
guanine + **5** → **20**	−19.06	−6.74	−2.29	0.46
8 → **10**	22.40	25.74	12.57	10.34
8 → **11**	4.66	7.87	0.10	1.57
18 → **21**	−0.67	0.21	−7.88	-4.39
18 → **22**	27.76	29.15	17.44	15.85
19 → **23**	−7.30	−4.87	−3.96	2.93
20 → **24**	8.63	11.60	8.42	9.50
guanine + **7** → **12**	4.43	7.21	14.11	14.91
12 → **13**	9.21	11.27	6.14	9.07

[a] Gas-phase energies calculated at the B3LYP/6-31+G (*28*) level of theory. [b] All energies were calculated at the gas-phase B3LYP/6-31+G (*28*) optimized geometries. Thermal enthalpy corrections and entropy terms were calculated from the B3LYP/6-31+G (*28*) harmonic vibrational frequencies. [c] Calculated using the conductor-like screening solvation model (COSMO) using the B3LYP/6-31+G (*28*) wave function. [d] Calculated using the Langevin Dipole solvent model (*34*) (ChemSol) using Merz−Kollman (*28*) atomic charges derived from the B3LYP/6-31G (*34*) wave function using the polarizable continuum model (*35*).

As shown in Scheme 2 for O^6-alkylation reactions between acrolein and guanine, the COSMO quantum chemical calculations predict that the conjugate addition reaction to form product **8** is favored ($\Delta G = 8.4$ kcal/mol) relative to direct addition to form product **9** ($\Delta G = 19.6$ kcal/mol). As described below, however, any of the three possible *N*-alkylation reactions is significantly favored

over the *O*-alkylations (Scheme 5, adducts **18**, **19**, and **20**).

After an initial α,*β*-conjugate addition, O^6-PAG (**8**) can undergo intramolecular cyclization via nucleophilic attack on the carbonyl to form one or more cyclic tautomers (**10** and **11**, Scheme 2). Interestingly, tautomer **11** with a seven-membered ring is favored over the six-membered ring **10**; however, both reactions **8** → **10** and **8** → **11** are endothermic.

For *N*-alkylation reactions between acrolein and guanine, Scheme 5 shows the possible alkylation products and their attendant cyclic tautomers. The three possible initial alkylation reactions are found to be very similar in energy, with reaction at N-7 (to give **20**) slightly favored over that at N-1 (to give **18**) or the exocyclic NH_2 (to give **19**). While intermediate **18** could cyclize to **21** or **22**, only **21** has been reported (*9*, *10*). This is in agreement with the COSMO and ChemSol predictions which show that the difference in free energies between the formations of **21** and **22** is 20−25 kcal/mol in favor of **21** (Table 3). Adduct **19** is found to have a favorable reaction energy to form **23**; in contrast, the cyclization of adduct **20** to give seven-membered ring **24** is predicted to have an unfavorable reaction free energy (Table 3).

The relative enthalpies for various conformers of **21** and **23** have been reported using semiempirical methods that find **21** is favored over **23** by about 1 kcal/mol when using gas-phase PM3 and AM1 calculations (*46*). The reverse is found using the MNDO formalism where the enthalpy of formation for **23** is 1.3 kcal/mol lower than that of **21** (*46*). The MNDO result is in close agreement with our more accurate ab initio quantum chemical, gas-phase, free energy calculations that show **23** to be lower in energy by 1.7 kcal/mol compared to **21** (Table 2). In the aqueous-phase, we predict the reverse of this ordering, with **21** being favored by 1.3 (ChemSol) to 2.0 (COSMO) kcal/mol (Table 2).

We also predicted the free energies for the reaction of chloroacetaldehyde (**7**) with guanine at the O^6 position as shown in Scheme 3. As with acrolein O^6-alkylation reactions, we find the O^6-alklyation by **7** to be energetically unfavored, with $\Delta G > 14$ kcal/mol. Similarly, a subsequent intramolecular cyclization to **13** is predicted to be endothermic.

In summary, the predicted free energies for the reactions of acrolein with guanine indicate that alkylations at the N-1, NH_2, and N-7 positions of guanine are favored over alkylation at O^6. Further, for the subsequent cyclization reactions, we predict that only the reactions to form cyclic products including N-1 and NH_2 (i.e., **21** and **23**) are energetically favored. This latter prediction correlates with in vitro experimental results: the major products isolated from reactions between acrolein and guanine are **21** and **23** (*9*, *10*). A comparison of the aqueous-phase free energies of **21** and **23** predict that **21** is slightly favored over **23**. The same order of favorability in the guanine adducts would not necessarily be found for guanosine analogues; however, it can be noted that only the guanosine analogue of **23** has been identified in the DNA of rodents and humans (*47*). The authors of this latter study stated that although their results suggested that the guanosine analogue of **23** was formed preferentially in vivo, it was possible that guanosine structures corresponding to **21** were not detected because they were more unstable or more efficiently repaired.

Conclusion

O^6-PAG (**8**) and O^6-EAG (**12**) were synthesized for use as authentic standards in our continuing investigations of DNA alkylation by acrolein and chloroacetaldehyde. Studies of the chemical stabilities of these adducts suggest that guanyl residues in DNA that have been alkylated by acrolein or chloroacetaldehyde will have lifetimes sufficient for detection. No experimental support was obtained for the formation of tautomeric structures from O^6-PAG or O^6-EAG.

Ab initio quantum chemical simulations of the free energies of reactions between acrolein and guanine indicate that *N*-alkylation is favored over O^6-alkylation and that subsequent cyclization reactions are most favorable if they involve the N-1 or NH_2 positions. When drawing conclusions from these data, however, it must be remembered that the calculated free energies reflect which reactions are thermodynamically favored. If there are significant energy barriers to these reactions, the actual product distribution could be different as a result of kinetic rather than thermodynamic control. Furthermore, the electronic changes that occur upon alkylation of guanine are not the same as those that derive from alkylation of N-9 substituted guanines (as in DNA). Predictions of relative product formation in DNA itself would be useful and, to this end, ab initio calculations of the type presented here are in progress for models of alkylated DNA.

We hypothesize that O^6-alkylation of guanine by acrolein will play a role in the mutagenicity associated with cyclophosphamide (and ifosfamide) therapy. The synthetic adducts reported here will be used to further investigations of this hypothesis.

Acknowledgment. We would like to thank Dr. Henry S. Friedman (Duke University Medical Center), Dr. Robert F. Struck (Southern Research Institute), and Dr. Anthony E. Pegg (The Milton S. Hershey Medical Center) for their contributions in recognizing the potential for alkylation of O^6-guanyl groups by acrolein. This work was supported in part by Public Health Service Grants CA68438 (S.M.L.), CA16783, CA692460, and CA52857 (O.M.C.), CA71627 (M.E.D.), and CA57725 (M.E.D.) from the National Cancer Institute (Department of Health and Human Resources) and by DAMD 17-99-1-9175 (M.P.G.). The work at Lawrence Livermore National Laboratory was performed under contract W-7405-ENG-48 from the U.S. Department of Energy. The NMR spectroscopy and mass spectrometry results were acquired through the Shared Instrumentation Facility of the Duke University Medical Center.

References

(1) Ludeman, S. M. (1999) The chemistry of the metabolites of cyclophosphamide. *Curr. Pharm. Des.* **5**, 627−643.

(2) Colvin, M., and Chabner B. A. (1991) Alkylating agents. In *Cancer Chemotherapy: Principles and Practice* (Chabner, B. A., and Collins, J. M., Eds.) pp 276−313, J. L. Lippincott, Philadelphia.

(3) Tolly, D. A. (1977) The effect of N-acetyl cysteine on cyclophosphamide cystitis. *Brit. J. Urol.* **49**, 659−661.

(4) Williams, M. L., and Wainer, I. W. (1999) Cyclophosphamide versus ifosfamide: "To use ifosfamide or not to use, that is the three dimensional question". *Curr. Pharm. Des.* **5**, 665−672.

(5) Kerbusch, T., de Kraker, J., Keizer, H. J., van Putten J. W. G., Groen, H. J. G., Jansen, R. L. H., Schellens, J. H. M., and Beijnen, J. H. (2001) Clinical pharmacokinetics and pharmacodynamics of ifosfamide and its metabolites. *Drug Dispos.* **40**, 41−62.

(6) Friedman, H. S., Pegg, A. E., Johnson, S. P., Loktionova, N. A., Dolan, M. E., Modrich, P., Moschel, R. C., Struck, R., Brent, T. P., Ludeman, S., Bullock, N., Kilborn, C., Keir, S., Dong, Q., and Bigner, D. D. (1999) Modulation of cyclophosphamide activity by O^6-alkylguanine-DNA alkyltransferase. *Cancer Chemother. Pharmacol.* **43**, 80−85.

(7) Cai, Y., Wu, M. H., Ludeman, S. M., Grdina, D. J., and Dolan, M. E. (1999) Role of O^6-alkylguanine-DNA alkyltransferase in protecting against cyclophosphamide-induced toxicity and mutagenicity. *Cancer Res.* **59**, 3059−3063.

(8) Clayden, J., Greeves, N., Warren, S., and Wothers, P. (2001) *Organic Chemistry*, pp 227−242, Oxford University Press, New York.

(9) Chung, F. L., Young, R., and Hecht, S. S. (1984) Formation of cyclic 1,N2-propanodeoxyguanosine adducts in DNA upon reaction with acrolein or crotonaldehyde. *Cancer Res.* **44**, 990−995.

(10) Eder, E., Hoffman, C., Bastian, H., Deininger, C., and Scheckenbach, S. (1990) Molecular mechanisms of DNA damage initiated by alpha, beta-unsaturated carbonyl compounds as criteria for genotoxicity and mutagenicity. *Environ. Health Perspect.* **88**, 99−106.

(11) Eder, E., and Hoffman, C. (1993) Identification and characterization of deoxyguanosine adducts of mutagenic beta-alkyl-substituted acrolein congeners. *Chem. Res. Toxicol.* **6**, 486-494.

(12) Eder, E., Scheckenbach, S., Deininger, C., and Hoffman, C. (1993) The possible role of alpha, beta-unsaturated carbonyl compounds in mutagenesis and carcinogenesis. *Toxicol. Lett.* **67**, 87−103.

(13) Hoffman, C., Bastian, H., Wiedenmann, M., Deininger, C., and Eder, E. (1989) Detection of acrolein congener-DNA adducts isolated from cellular systems. *Arch. Toxicol. Suppl.* **13**, 219−223.

(14) Khullar, S., Varaprasad, C. V., and Johnson, F. (1999) Postsynthetic generation of a major acrolein adduct of 2′-deoxyguanosine in oligomeric DNA. *J. Med. Chem.* **42**, 947−950.

(15) Nechev, L. V., Harris, C. M., and Harris, T. M. (2000) Synthesis of nucleosides and oligonucleotides containing adducts of acrolein and vinyl chloride. *Chem. Res. Toxicol.* **13**, 421−429.

(16) VanderVeen, L. A., Hashim, M. F., Nechev, L. V., Harris, T. M., Harris, C. M., and Marnett, L. J. (2001) Evaluation of the mutagenic potential of the principal DNA adduct of acrolein. *J. Biol. Chem.* **276**, 9066−9070.

(17) Yang, I. Y., Hossain, M., Miller, H., Khullar, S., Johnson, F., Grollman, A., and Moriya, M. (2001) Responses to the major acrolein-derived deoxyguanosine adduct in Escherichia coli. *J. Biol. Chem.* **276**, 9071−9076.

(18) Wang, M., McIntee, E. J., Cheng, G., Shi, Y., Villalta, P. W., and Hecht, S. S. (2001) A Schiff base is a major DNA adduct of crotonaldehyde. *Proc. Am. Assoc. Cancer Res.* **42**, 2544.

(19) Eder, E., Lutz, D., and Jorns, M. (1987) Allylic compounds bind directly to DNA: Investigation of the binding mechanisms in vitro. *Chem.-Biol. Interact.* **61**, 97−108.

(20) Griffin, R. J., Arris, C. E., Bleasdale, C., Boyle, F. T., Calvert, A. H., Curtin, N. J., Dalby, C., Kanugula, S., Lembicz, N. K., Newell, D. R., Pegg, A. E., and Golding, B. T. (2000) Resistance-modifying agents. 8. Inhibition of O^6-alkylguanine-DNA alkyltransferase by O^6-alkenyl-, O^6-cycloalkenyl-, and O^6-(2- oxoalkyl)guanines and potentiation of temozolomide cytotoxicity in vitro by O^6-(1-cyclopentenylmethyl)guanine. *J. Med. Chem.* **43**, 4071−4083.

(21) Chae, M. Y., McDougall, M. G., Dolan, M. E., Swenn, K., Pegg, A. E., and Moschel, R. C. (1994) Substituted O^6-benzylguanine derivatives and their inactivation of human O^6-alkylguanine-DNA alkyltransferase. *J. Med. Chem.* **37**, 342−347.

(22) Moschel, R. C., McDougall, M. G., Dolan, M. E., Stine, L., and Pegg, A. E. (1992) Structural features of substituted purine derivatives compatible with depletion of human O^6-alkylguanine-DNA alkyltransferase. *J. Med. Chem.* **35**, 4486-4491.

(23) Thaisrivongs, S., Pals, D. T., Turner, S. R., and Kroll, L. T. (1988) Conformationally constrained renin inhibitory peptides: gamma-lactam-bridged dipeptide isostere as conformational restriction. *J. Med. Chem.* **31**, 1369−1376.

(24) Zon, G., Ludeman, S. M., Sweet, E. M., Egan, W., and Phillips, L. R. (1982) *O*-Methylhydroxylamine as a new trapping reagent for quantitative studies of 4-hydroxycyclophosphamide and aldophosphamide. *J. Pharm. Sci.* **71**, 443−446.

(25) Eder, E. (2001) University of Wurzburg, Germany, personal communication. The NMR data listed in ref 19 likely contains a typographical error for the assignment of the C-8 proton in O^6-allylguanine.

(26) Becke, A. D. (1993) Density-functional thermochemistry. III. The role of exact exchange. *J. Chem. Phys.* **98**, 5648−5652.

(27) Lee, C., Yang, W., and Parr, R. G. (1988) Development of the Colle-Salvetti correlation-energy formula into a functional of the electron density. *Phys. Rev. B* **37**, 785−789.

(28) Besler, B. H., Merz, K. M., and Kollman, P. (1990) Atomic charges derived from semiempirical methods. *J. Comput. Chem.* **11**, 431−439.

(29) Jensen, F. (1999) *Introduction to Computational Chemistry*, John Wiley and Sons, New York.

(30) Barone, V., and Cossi, M. (1998) Quantum calculation of molecular energies and energy gradients in solution by a conductor solvent model. *J. Phys. Chem. A* **102**, 1995−2001.

(31) Tran, N. L., and Colvin, M. E. (2000) The prediction of biochemical acid dissociation constants using first principles quantum chemical simulations. *J. Mol. Structure, Theochem.* **532**, 127−137.

(32) Schuurmann, G. (2000) Prediction of Henry's law constant of benzene derivatives using quantum chemical continuum-solvation models. *J. Comput. Chem.* **21**, 17−34.

(33) Alagona, G., Ghio, C., Nagy, P. I., and Durant, G. J. (1999) Theoretical studies on the continuum solvation of some N,N′-dimethyl- and N-methyl-N′-acetyl-guanidine and guanidinium conformers. *J. Phys. Chem. A* **103**, 1857−1867.

(34) Florian, J., and Warshel, A. (1997) Langevin dipoles model for ab initio calculations of chemical processes in solution: Parametrization and application to hydration free energies of neutral and ionic solutes and conformational analysis in aqueous solution. *J. Phys. Chem. B* **101**, 5583−5595.

(35) Cossi, M., Barone, V., Cammi, R., and Tomasi, J. (1996) Ab initio study of solvated molecules: A new implementation of the polarizable continuum model. *Chem. Phys. Lett.* **255**, 327−335.

(36) Frisch, M. J., Trucks, G. W., Schlegel, H. B., Scuseria, G. E., Robb, M. A., and Cheeseman, J. R., et al. (1998) *Gaussian 98*, Revision A.4, Gaussian Inc., Pittsburgh.

(37) Frihart, C., and Leonard, N. (1973) Allylic rearrangement from O6 to C-8 in the Guanine Series. *J. Am. Chem. Soc.* **95**, 7174−7175.

(38) Zon, G., Ludeman, S. M., Brandt, J. A., Boyd, V. L., Ozkan, G., Egan, W., and Shao, K.-L. (1984) NMR spectroscopic studies of intermediary metabolites of cyclophosphamide. A comprehensive kinetic analysis of the interconversion of cis- and trans-4-hydroxycyclophosphamide with aldophosphamide and the concomitant partitioning of aldophosphamide between irreversible fragmentation and reversible conjugation pathways. *J. Med. Chem.* **27**, 466−485.

(39) Borch, R. F., and Getman, K. M. (1984) Base-catalyzed hydrolysis of 4-hydroperoxycyclophosphamide: Evidence for iminocyclophosphamide as an intermediate. *J. Med. Chem.* **27**, 485−490.

(40) Kwon, C. H., Maddison, K., LoCastro, L., and Borch, R. F. (1987) Accelerated decomposition of 4-hydroxycyclophosphamide by human serum albumin. *Cancer Res.* **47**, 1505−1508.

(41) Low, J. E., Borch, R. F., and Sladek, N. E. (1983) Further studies on the conversion of 4-hydroxyoxazaphosphorines to reactive mustards and acrolein in inorganic buffers. *Cancer Res.* **43**, 5815−5820.

(42) Borch, R. F., and Millard, J. A. (1987) The mechanism of activation of 4-hydroxycyclophosphamide. *J. Med. Chem.* **30**, 427−431.

(43) Dirven, H. A., Venekamp, J. C., van Ommen, B., and van Bladeren, P. J. (1994) The interaction of glutathione with 4-hydroxycyclophosphamide and phosphoramide mustard, studied by 31P nuclear magnetic resonance spectroscopy. *Chem.-Biol. Interact.* **93**, 185−196.

(44) Cai, Y., Wu, M. H., Xu-Welliver, M., Pegg, A. E., Ludeman, S. M., and Dolan, M. E. (2000) Effect of O^6-benzylguanine on alkylating agent-induced toxicity and mutagenicity in Chinese hamster ovary cells expressing wild-type and mutant O^6-alkylguanine-DNA alkyltransferases. *Cancer Res.* **60**, 5464−5469.

(45) Ludeman, S. M., Shulman-Roskes, E. M., Wong, K. K., Han, S. Y., Anderson, L. W., Strong, J. M., and Colvin, O. M. (1995) Oxime derivatives of the intermediary oncostatic metabolites of cyclophosphamide and ifosfamide: Synthesis and deuterium labeling for applications to metabolite quantification. *J. Pharm. Sci.* **84**, 393−398.

(46) Boerth, D. W., Eder, E., Hussain, S., and Hoffman, C. (1998) Structures of acrolein-guanine adducts: A semi-empirical self-consistent field and nuclear magnetic resonance spectral study. *Chem. Res. Toxicol.* **11**, 284−294.

(47) Nath, R. G., and Chung, F.-L. (1994) Detection of exocyclic 1,N^6-propanodeoxyguanosine adducts as common DNA lesions in rodents and humans. *Proc. Natl. Acad. Sci. U.S.A.* **91**, 7491−7495.

TX0101503